



UWL REPOSITORY

repository.uwl.ac.uk

Comprehensive analysis of transcriptomics and metabolomics to understand the flesh quality regulation of crucian carp (*Carassius auratus*) treated with short term micro-flowing water system

Du, H, Xiong, S, Lv, H, Zhao, S and Manyande, Anne ORCID logo <https://orcid.org/0000-0002-8257-0722> (2021) Comprehensive analysis of transcriptomics and metabolomics to understand the flesh quality regulation of crucian carp (*Carassius auratus*) treated with short term micro-flowing water system. Food Research International, 147. p. 110519. ISSN 0963-9969

<http://dx.doi.org/10.1016/j.foodres.2021.110519>

This is the Accepted Version of the final output.

UWL repository link: <https://repository.uwl.ac.uk/id/eprint/7957/>

Alternative formats: If you require this document in an alternative format, please contact: open.research@uwl.ac.uk

Copyright: Creative Commons: Attribution-Noncommercial-No Derivative Works 4.0

Copyright and moral rights for the publications made accessible in the public portal are retained by the authors and/or other copyright owners and it is a condition of accessing publications that users recognise and abide by the legal requirements associated with these rights.

Take down policy: If you believe that this document breaches copyright, please contact us at open.research@uwl.ac.uk providing details, and we will remove access to the work immediately and investigate your claim.

1 **Comprehensive analysis of transcriptomics and metabolomics to understand the flesh**
2 **quality regulation of crucian carp (*Carassius auratus*) treated with short term micro-flowing**
3 **water system**

4 Hongying Du^{a, b}; Shanbai Xiong^{a, b, *}; Hao Lv^a; Siming Zhao^{a, b}; Anne Manyande^c

6 ^a Key Laboratory of Environment Correlative Dietology, Ministry of Education, College of Food
7 Science and Technology, Huazhong Agricultural University, Wuhan, Hubei, P.R. China

8 ^b National R & D Branch Center for Conventional Freshwater Fish Processing, Wuhan, Hubei
9 430070, P.R. China

10 ^c School of Human and Social Sciences, University of West London, Middlesex TW8 9GA, UK

13 * Corresponding author

14 **Shanbai Xiong**: Email: xionsb@mail.hzau.edu.cn; Phone: 86-27-87288375;

Abstract

The short term micro-flowing purification system (STMFPS) has been shown to improve the flesh quality of freshwater fish. However, few studies have focused on the involved underlying mechanisms. This study explored the effect of STMFPS on the flesh quality of market-size freshwater fish based on the combination of metabolomics and transcriptomics methods. The UPLC-QTOF/MS based metabolomics method was utilized to screen metabolites and predict the possible major metabolic pathways during different STMFPS treatment periods (0 d, 1 d, 5 d and 9 d). Furthermore, the transcriptomic data demonstrated that the differentially expressed genes detected in crucian carp muscle were 2915, 7852 and 7183 after 1 d, 5 d and 9 d STMFPS treatment. Results showed that the TCA cycle, ornithine cycle, purine metabolism and amino acid catabolism play important roles in improving the flesh quality of crucian carp. This study may help to understand the mechanism of improving the flesh quality of aquatic products using STMFPS.

Keywords: Freshwater fish, Mass spectrometry (MS); Genes; Metabolites; Principal component analysis (PCA); Orthogonal partial least squares discriminant analysis (OPLS-DA)

1. Introduction

Crucian carp (*Carassius auratus*) is an omnivorous and important economic freshwater fish which is widely farmed in China (Ling et al., 2019), due to its palatability, fast growth rate, and high nutritional quality (Cui et al., 2020; Wu, 2020). The aquaculture of crucian carp has rapidly grown over the last two decades, and it has become one of the most important economic sources in China. Currently, high-density cultivation is the most popular method used for crucian carp production (Su, Luo, Jiao, & Wu, 2017). However, the rearing conditions or cultivation of microorganisms in aquatic environments could easily result in the accumulation of undesirable flavors in the fish, which in turn would affect to some extent the degree of acceptance by consumers of the crucian carp (Fuentes, Fernández-Segovia, Serra, & Barat, 2010; Rincón et al., 2016). In other words, the quality of crucian carp could have obvious disadvantages, such as loose muscle tissue, poorer taste *etc.* (Grigorakis, Taylor, & Alexis, 2003). In order to solve the poor quality of farmed freshwater fish under high-density cultivation, a variety of depuration treatments are used to improve the quality and acceptability of market-size fish before sales. The quality of numerous kinds of fish was significantly improved by depuration or purging and recirculating aquaculture systems, including halibut (Drake, DRAKE, Sanderson, Daniels, & Yates, 2010), atlantic salmon (Burr, Wolters, Schrader, & Summerfelt, 2012), rainbow trout (Schrader, Davidson, & Summerfelt, 2013), common carp (Zajic, Mraz, Sampels, & Pickova, 2013), grass carp (Lv, Hu, Xiong, You, & Fan, 2018) and so on. But there are few studies that have reported the mechanism which improved fish flesh quality by the depuration system treatment, thus further researches are still needed.

Metabolomics is the study of metabolites within organic tissues and biofluids to comprehensively identify and quantify all endogenous and exogenous low-molecular-weight

($<1000\ m/z$) molecules in a high-throughput manner, for observing the changes of the small molecules with metabolic fingerprinting (changes of the metabolic patterns) or metabolic profiling (changes of a group of metabolites or a specific pathway) due to endogenous and exogenous factors (Feizi, Hashemi-Nasab, Golpelichi, Sabourouh, & Parastar, 2021; Johnson, Sidwick, Pirgozliev, Edge, & Thompson, 2019). Metabolomics has been extensively applied to food sciences with two major aims, including the development of accurate and rapid food quality control methods and investigation of nutritional effects of selected foods or food components (Gil, 2017). Non-targeted metabolomics focus on finding as many small molecules as possible and global metabolic profiles, so that they are particularly useful when differences between sample sets are very small, or finding which compounds or classes of compounds are affected by the factor under investigation with various detection technologies, such as nuclear magnetic resonance spectroscopy (NMR) (Labine & Simpson, 2020), mass spectrometry (MS), *etc.* (Torres Santiago, Serrano Contreras, Meléndez Camargo, & Zepeda Vallejo, 2019; Zhu et al., 2019). Among these different kinds of detection technologies, the NMR-based method is a valuable tool for quantitatively identifying the different metabolites in tissues, due to advantages, such as highly reproducible, minimal sample preparation steps, nonrequirement of standards and qualitative and quantitative measurement (Labine & Simpson, 2020). Compared with the NMR-based method, the MS-based methods could offer higher sensitivity than the NMR and also require much fewer samples (Sugimoto, Kawakami, Robert, Soga, & Tomita, 2012). Currently, several types of MS techniques have been widely used in metabolomics analysis, such as liquid chromatography-mass spectrometry (LC-MS) and gas chromatography–mass spectrometry (GC-MS). Among these, LC-MS represented by UHPLC-Q-TOF-MS and UHPLC-Q-Orbitrap HRMS dominates the metabolomics arena due to its high resolution and

sensitivity (Wang et al., 2014). Therefore, LC-MS based metabolomics fingerprinting approaches have advantages on the evaluation of metabolic differences during various environmental systems or feeding modes of aquatic products based on metabolic patterns and correlation with the alteration of certain metabolic pathways (Cappello et al., 2016; Gika, Virgiliou, Theodoridis, Plumb, & Wilson, 2019; Zhang et al., 2019).

Transcriptomics is a high performance method used to study the differences which are implicit in fish living in different environments at the mRNA level. Transcriptomics analysis can effectively screen the differentially expressed genes (DEGs) of fish exposed to various environmental pollutants (Zhang et al., 2019), pathogenic microbial invasion (Long et al., 2015), stress responses (Petitjean et al., 2019) and their corresponding mechanisms. For example, short-term 17 α -ethynylestradiol exposure in sardine (*Sardinops sagax*) and mackerel (*Scomber japonicus*) disrupted the basic biological processes and pathways and the corresponding diagnostic biomarkers that monitor ocean environmental health were uncovered through transcriptomic analysis (Renaud et al., 2019). Transcriptomics sequencing explores the mechanism of Grass carp reovirus infection, which is involved in adsorption at the cell surface, followed by endocytosis into cells, transport of lysosomes which eventually results in cell necrosis and/or apoptosis (Chen et al., 2018). A former study (Sánchez et al., 2011) used transcriptomics to examine gene expression in different organs of rainbow trout caused by temperature, salinity, crowding and hypoxia, a change of single nucleotide polymorphism. The transcriptomic method has been applied to study the effects of long term starvation and diet composition on the expression of mitochondrial oxidative phosphorylation gene expression in gilthead sea bream (Silva-Marrero et al., 2017). In addition, transcriptomics can be used to determine the ecological diversity, genetic diversity and evolution of fish (Hughes et al.,

2017; Sin-Yeon et al., 2017). Therefore, the application of transcriptomics to the analysis of genes related to metabolic differences in the purification process of freshwater fish can clarify the regulatory mechanism of the purification treatment that improves the quality of freshwater fish.

In the present study, metabolomics and transcriptomic responses in the flesh of market-size crucian carp under treatment with short term micro-flowing purification system (STMFPS) were investigated for up to 9 days and then the possible representative metabolites and different signal pathways involved in the improvement of flesh quality for crucian carp were examined.

2. Materials and Methods

2.1 Chemical reagents

HPLC grade 2-Chloro-L-phenylalanine, methanol, acetonitrile and formic acid were obtained from Sigma Aldrich (St. Louis, MO, USA). Biochemical reagent creatinine was purchased in Biosharp (Hefei, Anhui, P.R. China). MS-222 (3-Aminobenzoic acid ethyl ester methanesulfonate) was obtained from Shanghai Yuanye Bio-Technology Co., Ltd (Shanghai, P.R. China), which was used to induce anesthesia in fresh crucian carp. The water used in all experiments was ultrapure water from a Milli-Q system (Millipore, Billerica, MA, USA). All chemical reagents used and water are chromatographic grade.

2.2 Experimental design structure

All animal standard operation procedures were approved by the Animal Care and Use Committee of Huazhong Agricultural University and performed in accordance with the Guidelines for Care and Use of Laboratory Animals of Huazhong Agricultural University. The whole experimental design procedures are illustrated in Fig. 1. Briefly, the freshwater fish were obtained

from Honghu city (Hubei, P.R. China) and transferred to the short term micro-flowing water system. The fish was depurated for different periods, and fresh muscle was obtained and extracted for the metabolomics and transcriptomics studies. The detailed information is provided below.

2.3 Fish sample preparation

The fresh crucian carp (250~400 g) from the freshwater fish farming area in Honghu Deyan Aquatic Product Company LTD were transported in troughs (Long × Width × Height: 7.0 m × 2.0 m × 0.8 m) with STMFPS. There were ~130 kg fish placed in each trough, the fish-water mass ratio was 1:30, and the water was continuously replaced with groundwater as the source of water supply. During the treatment period, the amount of water changed in each trough was about 15.6 m³/d, around 400% (v/v), the temperature of water was 19.0±0.6 °C, and all fish were deprived of food during the whole period. During the period of depuration, five crucian carps of similar size were randomly collected at every period of 0 d, 1 d, 5 d, 9 d. The sampled fish was anaesthetized using the anesthetic MS - 222 (100 mg/L) and was unconscious before slaughter. Fish were immediately gutted and segmented. At the end, the dorsal muscle of each fish was taken and immediately frozen with liquid nitrogen and stored at -80 °C for further analysis.

2.4 Metabolites extraction and UPLC-QTOF-MS based metabolomics analysis

The fish muscle samples (~50 mg) were extracted with methanol. Briefly, methanol (800 µL) and the internal standard 2-chlorophenylalanine (2.8 mg/mL, 10 µL) were added to the sample. Then, all fish samples were grinded for 90 s at 65 Hz, vortexed for 30 s and centrifuged for 15 min (12000 rpm, 4 °C).

The Acquity UPLC-QTOF system was used to separate and detect the metabolites of fish sample. The UPLC system was equipped with a binary pump, micro degasser, an autosampler and a

temperature-controlled column compartment. Chromatographic separations were performed on an ACQUITY UPLC HSS T3 column (1.8 μ m, 2.1 mm \times 100 mm; Waters, Ireland). 200 μ L supernatant was transferred to sample vials for UPLC-MS platform analysis, and compounds were eluted using a binary phase at a flow rate of 0.35 mL/min, where solvent A was water containing 0.1% formic acid (v/v) and solvent B was acetonitrile containing 0.1% formic acid (v/v). The following linear gradient elution program was used: 0-2 min, 95% A; 2-12 min, 95–5% A; 12-15 min, 5% A; 15-17 min, 5–95% A; 17-20 min, 95% A. The column was maintained at 40 °C and the injection volume was 0.6 μ L. To avoid the effects of fluctuations in instrument detection signals, samples were analyzed in random order. At the same time, quality control (QC) samples, which were prepared by mixing all the samples, were inserted into the sample queue to monitor system stability and ensure reliability of experimental data. The separated components were detected with a Xevo® G2-S QToF mass spectrometer (Waters Corp., Mil-ford, MA, USA) operating in negative and positive electrospray ionization (ESI) mode. Both ESI ion modes and conditions were collected as follows: Cone gas, 50 L/h; Ion source temperature, 120 °C (+)/110 °C(–); Desolvation gas temperature, 350 °C; Capillary voltage, 1.4 kV(ESI+)/1.3 kV(ESI–); Sample cone, 40 V(ESI+) or 23 V(ESI–); Gas flow, 600 L/h; Collision energy, 10–40 V; Ion energy: 1 V; Scan time: 0.03 s; Inter scan time: 0.2 s; Scan range 50–1500 m/z(Wang et al., 2019).

The raw data of UPLC-QTOF/MS were converted into *mzML* format using ProteoWizard, and XCMS was successively processed by peak alignment, peak detection, peak picking, peak filling, isotope elimination, normalization and peak area extraction. Then, principal component analysis (PCA) and orthogonal partial least squares discriminant analysis (OPLS-DA) of metabolome data was performed in SIMCA-P 13.0 software (Umetrics AB, Umea, Sweden). With the data from both

ionization modes, the supervised multivariate data analysis approach OPLS-DA was used to screen the significant different metabolites among the crucian carp samples in various purification periods. A statistically explicit threshold based on the variable importance of projection (VIP) and the student's *t*-tests (*p*-value) were used to identify metabolites with significant differences between the control and STMFPS treated groups. The corresponding metabolic pathways analysis were conducted using the MetaboAnalyst 4.0 software (<http://www.metaboanalyst.ca/>).

2.5 RNA extraction and transcriptomic analysis

To explore changes in mRNA levels of crucian carp after STMFPS treatment, fish samples (0 d, 1 d, 5 d, 9 d, *n* = 5 for every group) depurated in troughs were collected and used for RNA extraction and RNA sequence analysis. The total RNA was isolated by TRIzol™ Reagent (Invitrogen, Carlsbad, CA, USA) according to the manufacturer's protocol. The TruSeq RNA sample preparation kit from Illumina (San Diego, CA, USA) was used for cDNA library preparation. The cDNA library construction and sequencing and RNA-seq library preparation were performed on an Agilent 2100 Bioanalyzer and ABI StepOnePlus™ Real-Time PCR System as described previously (Trapnell et al., 2012). The obtained raw reads were cleaned by removing reads adapter sequences, ploy-N strands and low-quality reads. High quality clean reads were used for transcriptome *de novo* assembly using Trinity software (Wagner, Fulton, & Henschel, 2016). Clean reads were aligned to carp (*Cyprinus carpio*) reference genome sequences by hierarchical indexing for spliced alignment of transcripts with the application of HISAT2 (Kim, Langmead, & Salzberg, 2015). Gene expression was calculated using fragments per kilobase of exon per million mapped reads (FRKM) approach. DESeq2 R package was utilized to illustrate the differential expressions between the control group and treated groups (Varet, Brillet-Guéguen, Coppée, & Dillies, 2016).

Genes with an adjusted p -value < 0.05 obtained by DESeq2 were assigned as DEGs. Volcano plots were drawn to exhibit the overall distribution of the DEGs in different treatment groups represented by red, green and blue dots. These DEGs were then used to perform enrichment analysis of the Gene Ontology (GO) ([http:// www.geneontology.org/](http://www.geneontology.org/)) and the Kyoto Encyclopedia of Genes and Genomes (KEGG) pathway annotations. Each treatment had five biological replicates.

2.6 Statistical analysis

Statistical analysis was performed with SPSS 22.0 (IBM, New York, USA) using one-way ANOVA. Significant differences between treatments were analyzed by Student's t -tests run in SPSS, p -value < 0.05 was considered statistically significant. A statistical power analysis was used to estimate the sample size for significant differences, which was implemented in freeware GPower (Erdfelder, Faul, & Buchner, 1996), and metabolite network was constructed based in KEGG pathways.

3. Results and discussion

3.1 UPLC-QTOF/MS analysis

To investigate the metabolite compositions during different purification periods, the non-targeted metabolite profiling of extracts was detected. The flesh samples were collected from the crucian carp under different purification periods (0 d, 1 d, 5 d and 9 d). The metabolites extracted from muscles were screened with UPLC-QTOF/MS. In order to show differences in spectra among different types of samples, a series of liquid chromatography are illustrated in Fig. S1A-S1D. Under optimized elution conditions of ultra-high performance liquid chromatography, the elution periods of the main period were around 0.9 min-3.6 min, 8.5 min-12.0 min, 13.0 min-16.5 min and ~18.0

min.

Based on m/z values and the standard libraries (METLIN, and HMDB – Human Metabolome Database) by comparison, there were 342 metabolites (Putatively annotated compounds (Sumner et al., 2007)) identified in the samples, including 71 amino acids and amino acid derivatives, 107 lipids, 52 nucleic acid hydrolysates and their derivatives, and 109 sugars and carbon sources chemicals. As examples, a series of EIC (extracted ion chromatograms, Fig. S1E-S1H) and MS spectra (Fig. S1I-S1L) were collected to show the steps of identification of metabolites, such as urea, pyruvate, retinol and vitamin D3. It was very clear to see that there exists obvious differences among TIC chromatograms from different types of samples. However, it was difficult to extract the potential different metabolic markers in fish samples by intuitively comparing the chromatograms from the purified and control samples. Thus, the application of PCA and the pattern recognition method (OPLS-DA) were used to visualize the characteristic changes.

3.2 Principal component analysis

To initially evaluate the differences among fish samples from different purification periods, a non-supervised multivariate analysis method, PCA was used to analyze the multidimensional data and provide a comprehensive view of the clustering among different samples.

The UPLC-QTOF/MS data under ES+ mode was first utilized to conduct an overview of the clustering models and search possible outliers among samples. After reducing dimensions of the metabolic data matrix by dropping unnecessary information, the first two principal components PC1 and PC2 were obtained for these four different groups. The total contribution of the first two major components was 49.2% of the variance for all variables, and the scatter plot for PC1 (34.4%) and PC2 (14.8%) is illustrated in Fig. 2A. It clearly can be seen that fish samples were clustered together

after five or nine days' purification. The one-day purification treatment also influenced the components of the samples, as the samples were disperse distributed in the 2D space, one sample was out of space, and the samples were not clustered with samples in the control group. Then, the PCA models of 0 d vs. 1 d, 0 d vs. 5 d, and 0 d vs. 9 d were further conducted and illustrated in Fig. 2B (PC1: 30.4%; PC2: 21.1%), 2C (PC1: 53.1%; PC2: 13.9%) and 2D (PC1: 43.4%; PC2: 17.1%), respectively. The results are similar to the findings in Fig. 2A. The statistical parameters (R^2 and Q^2) of all PCA models are collected in Table 1. To screen the different metabolites among the control and treatment groups with short-term purification periods, the different metabolites were further explored with OPLS-DA methods.

3.3 OPLS-DA analysis

The OPLS-DA models were achieved by making comparisons between 0 d vs. 1 d; 0 d vs. 5 d and 0 d vs. 9 d. The evaluation parameters of these models (R^2Y and Q^2) are demonstrated in Table 1. The permutation test plots from the OPLS-DA models based on the positive ion mode are illustrated in Fig. 2E-2G. The models for comparisons of 0 d vs. 5 d and 0 d vs. 9 d under positive and negative ion mode data showed that the classification models were stable and reliable (R^2 and $Q^2 \geq 0.5$). The values of R^2Y sufficiently explained the differences between these two groups and the values of Q^2 indicate the predictive abilities of the constructed classification models. Furthermore, the models for comparisons of 0 d vs. 1 d under different ion modes explained the differences between these two groups ($R^2Y > 0.9$), but there was over-fitting in the negative ion mode ($Q^2 < 0.5$).

3.4 Identification of different metabolites of crucian carp during STMFPS treatment

The different metabolic patterns between every comparison were recognized according to their VIP > 1.5 and $p < 0.05$ values. Finally, the metabolic numbers for these three different comparisons

(0d vs. 1d, 0d vs. 5d and 0d vs. 9d) were 22, 81 and 64 of various metabolites, respectively. To analyze the efficiency of the short-term purification treatment, the different metabolites under two different periods were annotated.

To further identify the biomarkers at different short-term purification periods, the different metabolites and their relative contents among different groups were identified and analyzed. The selected metabolites were identified using *m/z* information of the metabolites and the Tandem MS database (METLIN and HMDB) and KEGG database. The identified results are shown in Table 2. Results of the statistical power were also calculated and displayed in this table, which was used to estimate the sample size to determine the significant difference (*: ≥ 0.8 for sufficient power validation). Finally, there were 10 metabolites which changed during the whole purification period; and 31 metabolites changed in two different treatment periods (Table 2). Changes can be seen in the types and contents of different metabolites of crucian carp muscles under different treatment periods.

The metabolic pathways that underwent significant changes during microfluidic treatment mainly include TCA cycle, ornithine cycle, purine metabolism and amino acid catabolism. Among them, the metabolic changes related to the TCA cycle mainly showed that pyruvate, succinic acid, and coenzyme *Q2* significantly decreased on days 5 and 9 after purification (as shown in Fig. 3A-3C) and AMP (Adenosine monophosphate) significantly increased after purification (Fig. 3D). The purine metabolism changes mainly indicated that the content of guanosine, guanine, and adenine increased significantly after 5 days' treatment (Fig. 3E-3G) and the content of ornithine, a product of purine catabolism, decreased significantly after 5 days of treatment (Fig. 3H). The difference in ornithine cycle metabolism is mainly due to the accumulation of oxalic acid and arginine succinic acid (Fig. 3I-3J) and the significant reduction in citrulline content after 5 days of microfluidic

treatment (Fig. 3K). The difference in amino acid metabolism is mainly manifested as changes in the content of free amino acids such as proline, tyrosine, tryptophan, and lysine after microfluidic treatment. Among them, the contents of serine and tyrosine increased after treatment, while the contents of tryptophan and lysine decreased. At the same time, a large amount of monoacylphospholipid molecules were observed during the microfluidic treatment process, indicating that the carp muscle phospholipid metabolism was active during the treatment process.

Due to changes in metabolites and the reported pathway of the metabolites in the KEGG database, the changes of the metabolic pathway of the crucian carp muscle during the short-term purification periods were obtained (Fig. 4). After the crucian carp was transferred from the aquaculture/transportation water to the STMFPS purified water, the ornithine cycle metabolism related to ammonia nitrogen excretion changed, at the same time, due to lack of food, the TCA cycle in the muscles of crucian carp weakened, causing changes in amino acid metabolism and purine metabolism to compensate for the required energy that maintain normal life activities. During this process, ornithine, arginine succinic acid and some purine nucleosides and purine bases accumulated affecting the flesh quality of crucian carp.

3.5 Metabolic mechanism of STMFPS to improve the flesh quality of crucian carp

Changes in differential metabolites of crucian carp indicate that the ornithine cycle metabolic pathway underwent significant changes during STMFPS treatment. Generally, seven key enzymes including carbamyl phosphate synthetase (CPS-1), ornithine carbamoyltransferase (OTC), spermine succinate synthetase (argininosuccinate synthetase, ASS), argininosuccinate lyase (ASL), arginase (arginase), N-acetyl glutamate synthetase (N- acetylglutamate synthetase) and ornithine aminotransferase (OAT) are involved in ornithine cycle metabolism in the animal body and

responsible for the synthesis of related substrates and related transport proteins for transmembrane transport (Morris, 2002).

When the crucian carp was transferred to clean water for a short period of treatment, with changes in ammonia nitrogen concentration gradient in the environment, the direct excretion of ammonia was inhibited and the activity of urea cycle-related enzymes and the synthesis of ornithine to citrulline rose, including CPS-1 in the liver and synthesis of arginine succinic acid in the liver and arginine succinate lyase (Saha & Ratha, 2007). Thus, the content of citrulline in muscle was significantly reduced, while the content of ornithine and arginine succinic acid increased. Ornithine in the body may also derive from the metabolism of glutamate and glutamine (Blachier, Boutry, Bos, & Tomé, 2009), and the synthesis and accumulation of glutamine is one of the defense mechanisms of freshwater fish against a high ammonia nitrogen environment. A study reported a similar finding that glutamine may accumulate in many tissues of crucian carp during the cultivation or transportation process (Zhang, Zhang, Wang, Gu, & Fan, 2017). As blood ammonia nitrogen levels decrease in STMFPS, glutamine produces ornithine under the action of glutaminase and P5C synthetase, which may be one of the major reasons for the increase in ornithine content in crucian carp flesh. Ornithine is an important flavor precursor and its derivative 1-pyrroline is one of the important substrates for Maillard reaction (Corral, Leitner, Siegmund, & Flores, 2016). Furthermore, ornithine can also reduce the bitterness of other amino acids in the food system to improve the flavor of food (Wan, Xiong, Zhang, & Zhu, 2013). Therefore, the accumulation of ornithine could be responsible for the enhancement of the crucian carp flavor during the STMFPS treatment.

3.6 Transcriptomics profiling and DEGs

The RNA-seq results indicate that the total number of genes expressed were distinct in the

control group and STMFPS-treated groups. In order to reflect the correlation of gene expression between the samples, the Pearson correlation coefficient of all gene expression levels between each of two different experimental groups was calculated. The correlation between the detected gene expression profiles of STMFPS-treated groups and control groups are presented in Fig. 5. The correlation is better when the correlation coefficient is closer to 1.00. Therefore, this figure could directly display the significant difference between the different treatment groups making the grouping clear. From Fig. 5, it can be seen that the correlation of samples between 0 d (control group) and 1 d was high ($p > 0.975$), indicating that the expression levels of different genes or transcriptomics profiling in the crucian carp muscles were similar. The correlation coefficients between the samples STMFPS-treated at 0 d and 5 d, 0 d and 9 d were low, demonstrating that the expression levels of various genes in crucian carp samples greatly changed after 5 d and 9 d STMFPS treatment.

Comparing with the control group, the DEGs were identified with the following statistical values for the genes: $p < 0.05$ and $|\log_2\text{FC (fold change)}| \geq 2$. The number of DEGs which overlapped between different STMFPS-treated periods and control groups are shown in the Venn diagram (Fig. 6A). Finally, there were 5917, 15085, 14183 DEGs identified between the 1 d, 5 d, 9 d STMFPS treated group and the control group (Ctr), and 3246 identical genes were found for these three different comparisons. The MA plots were drawn to intuitively represent the DEGs distribution or the degree of variation of these DEGs between different STMFPS treated and control groups (Fig. 6B). The abscissa represents A value (Average log CPM, \log_2 (counts -per-million)) used to measure the amount of gene expression. Vertical axis represents the M value ($\log_2\text{FC}$) used to estimate the up- and down-regulation of gene expression. The red dots indicate the upregulated expressed genes

($|\log_2FC(\text{fold change})| \geq 2, q \leq 0.001$), the blue dots represent the downregulated expressed genes ($\log_2FC(\text{fold change}) \leq -2, q \leq 0.001$), and the grey dots, the nondifferential expressed genes ($|\log_2FC(\text{fold change})| \leq 2, q > 0.001$). As it can be seen from Fig. 6B, compared with the untreated samples, most of DEGs in the crucian carp muscle samples after STMFPS treatment were up-regulated and the number of up-regulated genes elevated to the highest level at 5 d STMFPS treatment. The M values of most DEGs are distributed in $-4 \sim 3$, $-4 \sim 6$ and $-4 \sim 5$ between the control groups versus 1 d, 5 d and 9 d STMFPS treated groups. The number of DEGs increased with the range of M values, so the number of DEGs between Ctr vs. Day5 was the largest during the STMFPS treatment. Results of transcriptomic analysis indicate that the STMFPS treatment affected the expression of many genes in the crucian carp muscle. Compared with the control group, there were 4776, 14174, 13211 upregulated genes and 1141, 911, 972 downregulated genes found for different STMFPS-treated groups (1 d, 5 d, 9 d), respectively.

The expression levels of genes of all samples (control, 1 d, 5 d and 9 d) were produced with five biological replicates per treatment and are shown in the clustered heatmap (Fig. 6C). The gene expression status of crucian carp muscles under different purification periods was mainly divided into two parts, the gene expression of crucian carp samples treated on 0 d and 1 d is very similar and the transcription profiling of crucian carp samples treated on 5 d and 9 d by STMFPS bear a resemblance. Furthermore, there exist a big difference between 5 d/9 d STMFPS treated crucian carp samples and 0 d/1 d samples in gene expression levels. Basically, the transcriptome profiles of three STMFPS treatment groups were different compared with the control group.

3.7 GO enrichment analyses of DEGs

The classification and enrichment of DEGs help us to understand the functional properties of

DEGs detected in crucian carp muscle samples during different STMFPS treatment periods. Generally, gene ontology (GO) can be classified into three functional categories, including the molecular function, cellular component and biological process (Chen et al., 2018). Results of the GO function classification of DEGs under different treatment periods are plotted in Fig. 7. It can be seen that the cellular process, single-organism process and metabolic process are the top three functional classes of DEGs during the STMFPS treatment. For the metabolic process, there were 1322, 3299, 3026 DEGs identified between the control and the other three different STMFPS treatment groups (1 d, 5 d and 9 d), respectively. Furthermore, it can clearly be noticed that the number of DEG in crucian carp flesh is affected by the period of STMFPS treatment. Moreover, the number of DEGs involved in the metabolic process in crucian carp flesh reached a maximum at 5 d STMFPS treatment, and then it tended to stabilize after 9 d STMFPS treatment.

3.8 KEGG Metabolic Pathway analysis of DEGs

In order to compare the transcriptome and metabolome data, the metabolic pathways of DEGs involved in the KEGG database were further analyzed. The detailed metabolic pathway and the corresponding number of DEGs of each metabolic pathway are listed in Table 3. As can be seen, purine metabolism, pyrimidine metabolism and glycerophospholipid metabolism represent the majority of metabolic pathways, which take up the top three number of DEGs between the control group and the other three STMFPS treatments groups. It means that STMFPS treatment mainly resulted in changes in nucleotide and phospholipid metabolism in the muscle of crucian carp flesh. Transcriptomics analysis indicates that STMFPS treatment can affect the purine metabolism of freshwater fish, which induced the accumulation of single nucleotides IMP and AMP in crucian carp flesh, reduced the content of xanthine, hypoxanthine and other single nucleotide degradation

products, thus affecting the flesh quality of freshwater fish. Therefore, the results of transcriptomics were in good accord with the results of metabolomics of crucian carp treated with STMFPS.

According to the results of DEGs in the metabolic classification, combined with the ornithine cycle-related metabolic pathways in the KEGG database, the expression of ornithine cycle-related genes was analyzed. The DEGs are shown in Table 4. It can be seen that the STMFPS treatment led to differential expression of seven enzyme genes related to the ornithine cycle in the flesh of crucian carp. Among these, the ornithine oxoaminotransferase gene was down-regulated and the other enzyme genes were up-regulated. The expressions of arginine succinate synthetase and arginine succinate lyase were up-regulated, which is in accordance with results of the metabolomics study, in other words, STMFPS induced citrulline and metabolized more arginine succinate in freshwater fish flesh. Furthermore, the upregulated genes of enzymes including N-alpha-acetyltransferase, pyrroline-5-carboxylate reductase, delta-1-pyrroline-5-carboxylate synthetase and carbamoyl-phosphate synthase were intermediate catalytic enzyme genes for the synthesis of ornithine by glutamic acid and proline, respectively. Therefore, the results of DEGs related to the ornithine cycle in this study support the results of changes in the content of related metabolites. In this regard, STMFPS treatment affected the ornithine cycle metabolic pathways in freshwater fish and led the content of ornithine and spermine aminosuccinic acid to increase significantly, however the contents of citrulline, proline, urea decreased significantly, thereby affecting the flesh quality of crucian carp.

4. Conclusion

In summary, the current integrative application of transcriptome and metabolome approaches has potential implications for understanding the effect of flesh quality improvement with STMFPS

treatment. UPLC-QTOF MS based metabolomics showed that STMFPS affected TCA cycle, ornithine cycle, purine metabolism, amino acid metabolism and fatty acid metabolism pathways in crucian carp flesh. Results of transcriptome were basically in agreement with the metabolome and to explore insights to understanding the flesh quality improvement of market size crucian carp, STMFPS treatment was used. Transcriptome showed that STMFPS treatment induced significant changes in various genes involved in purine and arginine metabolism pathways. These results provided some information for understanding the main metabolic mechanism for improving the flesh quality of crucian carp of STMFPS treatment.

Credit authorship contribution statement

Hongying Du: Investigation, Writing - original draft and review, Formal analysis, Visualization, Conceptualization, Funding acquisition; **Shanbai Xiong:** Funding acquisition, Supervision, Conceptualization; **Hao Lv:** Investigation, Formal analysis, Validation, Methodology; **Siming Zhao:** Investigation; **Anne Manyande:** Writing - review & editing.

Conflict of interest

The authors declare that there is no conflict of interest

Acknowledgement All authors express their appreciation to Dr. Yunlong Wang and Dr. Jianxun Zhou from the Shanghai Sensichip Infotech Co. (Shanghai, China) for the detection of the samples. This research was financially supported by the Agriculture Research System of China (CARS-45-28); the National Natural Science Foundation of China (No. 31772047), and the Fundamental

Research Funds for the Central Universities of China (No. 2662019PY031 and 2662017PY021).

References

- Blachier, F., Boutry, C., Bos, C., & Tomé, D. (2009). Metabolism and functions of l-glutamate in the epithelial cells of the small and large intestines. *The American Journal of Clinical Nutrition*, 90(3), 814S-821S. doi: <https://doi.org/10.3945/ajcn.2009.27462S>
- Burr, G. S., Wolters, W. R., Schrader, K. K., & Summerfelt, S. T. (2012). Impact of depuration of earthy-musty off-flavors on fillet quality of Atlantic salmon, *Salmo salar*, cultured in a recirculating aquaculture system. *Aquacultural Engineering*, 50, 28-36. doi: <https://doi.org/10.1016/j.aquaeng.2012.03.002>
- Cappello, T., Brandão, F., Guilherme, S., Santos, M. A., Maisano, M., Mauceri, A., . . . Pereira, P. (2016). Insights into the mechanisms underlying mercury-induced oxidative stress in gills of wild fish (*Liza aurata*) combining 1H NMR metabolomics and conventional biochemical assays. *Science of The Total Environment*, 548-549, 13-24. doi: <https://doi.org/10.1016/j.scitotenv.2016.01.008>
- Chen, G., He, L., Luo, L., Huang, R., Liao, L., Li, Y., . . . Wang, Y. (2018). Transcriptomics Sequencing Provides Insights into Understanding the Mechanism of Grass Carp Reovirus Infection. *International Journal of Molecular Sciences*, 19(2), 488-498. doi: <https://doi.org/10.3390/ijms19020488>
- Corral, S., Leitner, E., Siegmund, B., & Flores, M. (2016). Determination of sulfur and nitrogen compounds during the processing of dry fermented sausages and their relation to amino acid generation. *Food Chemistry*, 190, 657-664. doi: <https://doi.org/10.1016/j.foodchem.2015.06.009>
- Cui, D., Zhang, P., Li, H., Zhang, Z., Luo, W., & Yang, Z. (2020). Biotransformation of dietary inorganic arsenic in a freshwater fish *Carassius auratus* and the unique association between arsenic dimethylation and oxidative damage. *Journal of Hazardous Materials*, 391, 122153. doi: <https://doi.org/10.1016/j.jhazmat.2020.122153>
- Drake, S. L., DRAKE, M. A., Sanderson, R., Daniels, H. V., & Yates, M. D. (2010). The effect of purging time on the sensory properties of aquacultured southern flounder (*paralichthys lethostigma*). *Journal of Sensory Studies*, 25(2), 246-259. doi: <https://doi.org/10.1111/j.1745-459X.2009.00255.x>
- Erdfelder, E., Faul, F., & Buchner, A. (1996). GPOWER: A general power analysis program. *Behavior Research Methods, Instruments, & Computers*, 28(1), 1-11. doi: <https://doi.org/10.3758/BF03203630>
- Feizi, N., Hashemi-Nasab, F. S., Golpelichi, F., Saburouh, N., & Parastar, H. (2021). Recent trends in application of chemometric methods for GC-MS and GC×GC-MS-based metabolomic studies. *TrAC Trends in Analytical Chemistry*, 138, 116239. doi: <https://doi.org/10.1016/j.trac.2021.116239>
- Fuentes, A., Fernández-Segovia, I., Serra, J. A., & Barat, J. M. (2010). Comparison of wild and cultured sea bass (*Dicentrarchus labrax*) quality. *Food Chemistry*, 119(4), 1514-1518. doi: <https://doi.org/10.1016/j.foodchem.2009.09.036>

- Gika, H., Virgiliou, C., Theodoridis, G., Plumb, R. S., & Wilson, I. D. (2019). Untargeted LC/MS-based metabolic phenotyping (metabonomics/metabolomics): The state of the art. *Journal of Chromatography B*, *1117*, 136-147. doi: <https://doi.org/10.1016/j.jchromb.2019.04.009>
- Gil, A. M. (2017). Metabonomics in Food Science. In J. C. Lindon, G. E. Tranter & D. W. Koppenaal (Eds.), *Encyclopedia of Spectroscopy and Spectrometry (Third Edition)* (pp. 790-796). Oxford: Academic Press.
- Grigorakis, K., Taylor, K. D. A., & Alexis, M. N. (2003). Organoleptic and volatile aroma compounds comparison of wild and cultured gilthead sea bream (*Sparus aurata*): sensory differences and possible chemical basis. *Aquaculture*, *225*(1), 109-119. doi: [https://doi.org/10.1016/S0044-8486\(03\)00283-7](https://doi.org/10.1016/S0044-8486(03)00283-7)
- Hughes, L. C., Somoza, G. M., Nguyen, B. N., Bernot, J. P., González-Castro, M., Díaz de Astarloa, J. M., & Ortí, G. (2017). Transcriptomic differentiation underlying marine-to-freshwater transitions in the South American silversides *Odontesthes argentinensis* and *O. bonariensis* (Atheriniformes). *Ecology and evolution*, *7*(14), 5258-5268. doi: <https://doi.org/10.1002/ece3.3133>
- Johnson, A. E., Sidwick, K. L., Pirgozliev, V. R., Edge, A., & Thompson, D. F. (2019). The use of metabonomics to uncover differences between the small molecule profiles of eggs from cage and barn housing systems. *Food Control*, *100*, 165-170. doi: <https://doi.org/10.1016/j.foodcont.2019.01.023>
- Kim, D., Langmead, B., & Salzberg, S. L. (2015). HISAT: a fast spliced aligner with low memory requirements. *Nature Methods*, *12*(4), 357-360. doi: <https://doi.org/10.1038/nmeth.3317>
- Labine, L. M., & Simpson, M. J. (2020). The use of nuclear magnetic resonance (NMR) and mass spectrometry (MS)-based metabolomics in environmental exposure assessment. *Current Opinion in Environmental Science & Health*, *15*, 7-15. doi: <https://doi.org/10.1016/j.coesh.2020.01.008>
- Ling, X.-d., Dong, W.-t., Zhang, Y., Qian, X., Zhang, W.-d., He, W.-h., . . . Liu, J.-x. (2019). Comparative transcriptomics and histopathological analysis of crucian carp infection by atypical *Aeromonas salmonicida*. *Fish & Shellfish Immunology*, *94*, 294-307. doi: <https://doi.org/10.1016/j.fsi.2019.09.006>
- Long, M., Zhao, J., Li, T., Tafalla, C., Zhang, Q., Wang, X., . . . Li, A. (2015). Transcriptomic and proteomic analyses of splenic immune mechanisms of rainbow trout (*Oncorhynchus mykiss*) infected by *Aeromonas salmonicida* subsp. *salmonicida*. *Journal of Proteomics*, *122*, 41-54. doi: <https://doi.org/10.1016/j.jprot.2015.03.031>
- Lv, H., Hu, W., Xiong, S., You, J., & Fan, Q. (2018). Depuration and starvation improves flesh quality of grass carp (*Ctenopharyngodon idella*). *Aquaculture Research*, *49*(9), 3196-3206. doi: <https://doi.org/10.1111/are.13784>
- Morris, S. M. (2002). Regulation of enzymes of the urea cycle and arginine metabolism. *Annual Review of Nutrition*, *22*(1), 87-105. doi: <https://doi.org/10.1146/annurev.nutr.22.110801.140547>
- Petitjean, Q., Jean, S., Gandar, A., Côte, J., Laffaille, P., & Jacquin, L. (2019). Stress responses in fish: From molecular to evolutionary processes. *Science of The Total Environment*, *684*, 371-380. doi: <https://doi.org/10.1016/j.scitotenv.2019.05.357>
- Renaud, L., Agarwal, N., Richards, D. J., Falcinelli, S., Hazard, E. S., Carnevali, O., . . . Hardiman, G. (2019). Transcriptomic analysis of short-term 17 α -ethynylestradiol exposure in two

482 Californian sentinel fish species sardine (*Sardinops sagax*) and mackerel (*Scomber*
483 *japonicus*). *Environmental Pollution*, *244*, 926-937. doi:
484 <https://doi.org/10.1016/j.envpol.2018.10.058>

485 Rincón, L., Castro, P. L., Álvarez, B., Hernández, M. D., Álvarez, A., Claret, A., . . . Ginés, R. (2016).
486 Differences in proximal and fatty acid profiles, sensory characteristics, texture, colour and
487 muscle cellularity between wild and farmed blackspot seabream (*Pagellus bogaraveo*).
488 *Aquaculture*, *451*, 195-204. doi: <https://doi.org/10.1016/j.aquaculture.2015.09.016>

489 Sánchez, C. C., Weber, G. M., Gao, G., Cleveland, B. M., Yao, J., & Rexroad, C. E. (2011). Generation
490 of a reference transcriptome for evaluating rainbow trout responses to various stressors.
491 *BMC Genomics*, *12*(1), 626-636. doi: <https://doi.org/10.1186/1471-2164-12-626>

492 Saha, N., & Ratha, B. K. (2007). Functional ureogenesis and adaptation to ammonia metabolism in
493 Indian freshwater air-breathing catfishes. *Fish Physiology & Biochemistry*, *33*(4), 283-295.
494 doi: <https://doi.org/10.1007/s10695-007-9172-3>

495 Schrader, K. K., Davidson, J. W., & Summerfelt, S. T. (2013). Evaluation of the impact of nitrate-
496 nitrogen levels in recirculating aquaculture systems on concentrations of the off-flavor
497 compounds geosmin and 2-methylisoborneol in water and rainbow trout (*Oncorhynchus*
498 *mykiss*). *Aquacultural Engineering*, *57*, 126-130. doi:
499 <https://doi.org/10.1016/j.aquaeng.2013.07.002>

500 Silva-Marrero, J. I., Sáez, A., Caballero-Solares, A., Viegas, I., Almajano, M. P., Fernández, F., . . .
501 Metón, I. (2017). A transcriptomic approach to study the effect of long-term starvation
502 and diet composition on the expression of mitochondrial oxidative phosphorylation genes
503 in gilthead sea bream (*Sparus aurata*). *BMC Genomics*, *18*(1), 768-779. doi:
504 <https://doi.org/10.1186/s12864-017-4148-x>

505 Sin-Yeon, Kim, Maria, M., Costa, Anna, . . . Velando. (2017). Transcriptional mechanisms underlying
506 life-history responses to climate change in the three-spined stickleback. *Evolutionary*
507 *Applications*, *10*, 718-730. doi: <https://doi.org/10.1111/eva.12487>

508 Su, J., Luo, Y., Jiao, X., & Wu, J. (2017). Effect of the ecological fish farming technique on the muscle
509 quality of crucian carp (*Carassius auratus*). *Journal of Aquaculture*, *38*(4), 22-25.

510 Sugimoto, M., Kawakami, M., Robert, M., Soga, T., & Tomita, M. (2012). Bioinformatics Tools for
511 Mass Spectroscopy-Based Metabolomic Data Processing and Analysis. *Current*
512 *Bioinformatics*, *7*(1), 96-108. doi: [Doi 10.2174/157489312799304431](https://doi.org/10.2174/157489312799304431)

513 Sumner, L. W., Amberg, A., Barrett, D., Beale, M. H., Beger, R., Daykin, C. A., . . . Viant, M. R. (2007).
514 Proposed minimum reporting standards for chemical analysis. *Metabolomics*, *3*(3), 211-
515 221. doi: [10.1007/s11306-007-0082-2](https://doi.org/10.1007/s11306-007-0082-2)

516 Torres Santiago, G., Serrano Contreras, J. I., Meléndez Camargo, M. E., & Zepeda Vallejo, L. G.
517 (2019). NMR-based metabolomic approach reveals changes in the urinary and fecal
518 metabolome caused by resveratrol. *Journal of Pharmaceutical and Biomedical Analysis*,
519 *162*, 234-241. doi: <https://doi.org/10.1016/j.jpba.2018.09.025>

520 Trapnell, C., Roberts, A., Goff, L., Pertea, G., Kim, D., Kelley, D. R., . . . Pachter, L. (2012). Differential
521 gene and transcript expression analysis of RNA-seq experiments with TopHat and
522 Cufflinks. *Nature Protocols*, *7*(3), 562-578. doi: <https://doi.org/10.1038/nprot.2012.016>

523 Varet, H., Brillet-Guéguen, L., Coppée, J. Y., & Dillies, M. A. (2016). SARTools: A DESeq2- and
524 EdgeR-Based R Pipeline for Comprehensive Differential Analysis of RNA-Seq Data. *Plos*
525 *One*, *11*, e0157022. doi: <https://doi.org/10.1371/journal.pone.0157022>

- Wagner, M., Fulton, B., & Henschel, R. (2016). *Performance Optimization for the Trinity RNA-Seq Assembler*, Cham, 29-40.
- Wan, H., Xiong, Y., Zhang, J., & Zhu, C. (2013). Research progress in products exploitation and application of L-ornithine. *China Brewing*, 32, 8-12. doi: [https://doi.org/0254-5071\(2013\)01-0008-05](https://doi.org/0254-5071(2013)01-0008-05)
- Wang, H., Li, S., Qi, L., Xu, W., Zeng, Y., Hou, Y., . . . Sun, C. (2014). Metabonomic analysis of quercetin against the toxicity of chronic exposure to low-level dichlorvos in rats via ultra-performance liquid chromatography–mass spectrometry. *Toxicology Letters*, 225(2), 230-239. doi: <https://doi.org/10.1016/j.toxlet.2013.12.017>
- Wang, Y., Li, C., Li, L., Yang, X., Chen, S., Wu, Y., . . . Yang, D. (2019). Application of UHPLC-Q/TOF-MS-based metabolomics in the evaluation of metabolites and taste quality of Chinese fish sauce (Yu-lu) during fermentation. *Food Chemistry*, 296(OCT.30), 132-141. doi: <https://doi.org/10.1016/j.foodchem.2019.05.043>
- Wu, S. (2020). Dietary Astragalus membranaceus polysaccharide ameliorates the growth performance and innate immunity of juvenile crucian carp (*Carassius auratus*). *International Journal of Biological Macromolecules*, 149, 877-881. doi: <https://doi.org/10.1016/j.ijbiomac.2020.02.005>
- Zajic, T., Mraz, J., Sampels, S., & Pickova, J. (2013). Fillet quality changes as a result of purging of common carp (*Cyprinus carpio* L.) with special regard to weight loss and lipid profile. *Aquaculture*, 400-401, 111-119. doi: <https://doi.org/10.1016/j.aquaculture.2013.03.004>
- Zhang, W., Tan, B., Ye, G., Wang, J., Dong, X., Yang, Q., . . . Zhang, H. (2019). Identification of potential biomarkers for soybean meal-induced enteritis in juvenile pearl gentian grouper, *Epinephelus lanceolatus* ♂ × *Epinephelus fuscoguttatus* ♀. *Aquaculture*, 512, 734337. doi: <https://doi.org/10.1016/j.aquaculture.2019.734337>
- Zhang, Y., Zhang, H., Wang, L., Gu, B., & Fan, Q. (2017). Impact factors of ammonia toxicity and strategies for ammonia tolerance in air-breathing fish: A review. *Acta Hydrobiologica Sinica*, 41(5), 1157-1167. doi: <https://doi.org/10.7541/2017.144>
- Zhu, H., Wang, Z., Wu, Y., Jiang, H., Zhou, F., Xie, X., . . . Hua, C. (2019). Untargeted metabonomics reveals intervention effects of chicory polysaccharide in a rat model of non-alcoholic fatty liver disease. *International Journal of Biological Macromolecules*, 128, 363-375. doi: <https://doi.org/10.1016/j.ijbiomac.2019.01.141>

Figure legends:

Fig. 1 Flow diagram of the experimental design.

Fig. 2 Results of PCA analysis (A-D) and the permutation test plots (E-G) from the OPLS-DA models for the metabolites detected using UPLC-QTOF/MS equipped with both ESI+ mod which were obtained from crucian carp muscle during different depuration periods. *Note: A: All samples in four groups; B: Control vs. 1 d; C: Control vs. 5 d; D: Control vs. 9 d; E: Control vs. 1 d; F: Control vs. 5 d; G: Control vs. 9 d. The criteria for validity of the OPLS-DA model are indicated as following: All blue Q^2 -values to the left are lower than the original points to the right; or the blue regression line of the Q^2 -plots intersected the vertical axis (on the left) or below zero.*

Fig. 3: Comparative contents of different metabolites in crucian carp muscle during the depuration procedure ("*": $p < 0.05$; "***": $p < 0.01$; "*****": $p < 0.001$). *Note: A-D: Related with energy metabolism; E-H: Related with the purine metabolic cycle; I-K: Related with the ornithine metabolic cycle.*

Fig. 4 Effect of the depuration on metabolic pathways of crucian carp muscle. *Note: Different colors of metabolites represent change of comparative content, red: increased; blue: did not significantly change; green: decreased.*

Fig. 5 Correlation heatmap of the Pearson correlation coefficient of all gene expressions in four different groups (Ctrl-Ctr5: Control; Day1: 1 d; Day5: 5 d; Day9: 9 d).

Fig. 6 (A) Venn diagram of significantly enriched DEGs in different group comparisons representing the unique and overlapping DEGs. (B) MA plot distribution of DEGs of crucian carp muscle during different depuration periods. The red and blue dots indicate that the genes were differently expressed, and the grey dots indicate that the genes were not differentially expressed. The positive and negative values represent the up- and downregulation of DEGs, respectively. (C) Clustered heatmap for DEGs detected from different groups with rows representing DEGs and columns representing samples. *Note: Columns represent every gene set that was significantly up-regulated (red) or down-regulated (blue) in different groups (Ctrl-Ctr5: Control; Day1: 1 d; Day5: 5 d; Day9: 9 d).*

Fig. 7 GO classification of DEGs. (A) GO functional classification of DEGs between control (Ctrl) and Day1. (B) GO functional classification of DEGs between Ctrl and Day5. (C) GO functional classification of DEGs between Ctrl and Day9. (Ctrl, Day1, Day5, Day9 represent 0 d, 1 d, 5 d and 9 d STMFPS treatment groups, respectively).

Table 1: Collection of parameters of PCA and OPLS-DA models for the comparisons of metabolites in crucian carp muscle treated at different depuration periods

| Ions modes | Comparisons | PCA | | OPLS-DA | | |
|------------|-------------|------------------|----------------|------------------|------------------|----------------|
| | | R ² X | Q ² | R ² X | R ² Y | Q ² |
| ESI+ | A vs. B | 0.705 | 0.112 | 0.386 | 0.944 | 0.648 |
| | A vs. C | 0.670 | 0.351 | 0.658 | 0.999 | 0.983 |
| | A vs. D | 0.611 | 0.341 | 0.543 | 0.999 | 0.972 |
| ESI- | A vs. B | 0.584 | -0.00327 | 0.238 | 0.997 | 0.287 |
| | A vs. C | 0.621 | 0.349 | 0.691 | 0.998 | 0.915 |
| | A vs. D | 0.547 | 0.234 | 0.494 | 0.998 | 0.961 |

(Note: A、B、C、D represents the different groups treated at different depuration periods, such as 0 d、1 d、5 d、9 d)

Table 2: Collection of different metabolites in crucian carp muscle during different depuration periods. Note, Data was calculated as the ratio of the relative concentrations of the metabolites between depurated samples and the control samples. A/B/C/D was represented the relative concentrations of samples under various depuration periods - 0/1/5/9 days; Different metabolites were screened out according to VIP values ($VIP > 1.5$) in the OPLS-DA models and p value in t-test ($p < 0.05$); *: The statistical power was bigger than 0.8.

| NO | Name | MW (Da) | Retention time(min) | Relative amount | | |
|----|-------------------------------------|------------|------------------------|-----------------|--------|--------|
| | | | | B/A | C/A | D/A |
| 1 | Urea | 60.03 | 15.540 | 0.227* | 0.039* | 0.051* |
| 2 | Pyruvate | 88.02 | 18.223 | 0.657* | 0.543* | 0.549* |
| 3 | Oxalic acid | 90.00 | 18.223 | 0.668 | 0.539* | 0.524* |
| 4 | Isovaleric acid | 102.07 | 15.529 | 0.116* | 0.032* | 0.038* |
| 5 | Ribitol | 152.07 | 15.530 | 0.117* | 0.023* | 0.026* |
| 6 | Citrulline | 175.10 | 15.530 | 0.110* | 0.014* | 0.015* |
| 7 | Retinol | 286.23 | 13.745 | 0.457* | 0.355* | 0.513* |
| 8 | Stearic acid | 284.27 | 13.002 | 0.490* | 0.498* | 0.595* |
| 9 | Vitamin D3 | 384.34 | 15.671 | 0.391* | 0.106* | 0.145* |
| 10 | LysoPE(0:0/20:0) | 509.35 | 11.536 | 1.285 | 1.246 | 1.539* |
| 11 | Thymine | 126.04 | 0.978 | 0.777 | | 0.668 |
| 12 | TXB2 | 370.24 | 14.021 | 0.756* | | 0.661* |
| 13 | LysoPE(0:0/22:2(13Z,16Z)) | 533.35 | 11.856 | 1.611 | | 1.648* |
| 14 | LysoPE(0:0/22:1(13Z)) | 535.36 | 12.322 | 1.441 | | 1.565* |
| 15 | Succinic acid | 118.03 | 18.186 | | 0.662* | 0.716* |
| 16 | Creatine | 131.07 | 3.443 | | 4.482* | 4.182* |
| 17 | Ornithine | 132.09 | 3.471 | | 6.264* | 6.017* |
| 18 | Caprylic acid | 144.12 | 1.884 | | 7.820* | 4.425* |
| 19 | L-Tyrosine | 181.07 | 3.446 | | 4.278* | 4.018* |
| 20 | D-Sorbitol | 182.08 | 11.463 | | 2.768* | 2.925* |
| 21 | L-Cystathionine | 222.07 | 11.391 | | 2.870* | 3.090* |
| 22 | L-Tryptophan | 204.09 | 11.209 | | 0.391* | 0.541* |
| 23 | Myristic acid | 228.21 | 11.595 | | 0.484* | 0.651* |
| 24 | Guanosine | 283.09 | 3.460 | | 7.524* | 6.447* |
| 25 | Argininosuccinic acid | 290.12 | 18.117 | | 1.834 | 1.766* |
| 26 | β -estradiol | 272.18 | 0.953 | | 3.156* | 2.703 |
| 27 | Alpha-CEHC | 278.15 | 11.442 | | 2.593* | 2.751* |
| 28 | Cortisone | 360.19 | 11.455 | | 1.756* | 1.880* |
| 29 | Adenosine monophosphate | 347.06 | 0.867 | | 3.489* | 1.869 |
| 30 | PGA1 | 336.23 | 11.447 | | 0.416* | 0.554* |
| 31 | Nutriacholic acid | 390.28 | 14.222 | | 0.490* | 0.537* |
| 32 | MG(0:0/22:5(4Z,7Z,10Z,13Z,16Z)/0:0) | 404.29 | 13.096 | | 0.603* | 0.610 |
| 33 | Vitamin D2 | 396.34 | 10.260 | | 2.702* | 2.869* |

| | | | | | |
|----|----------------------------------|--------|--------|--------|--------|
| 34 | LysoPE(0:0/14:0) | 425.25 | 9.817 | 0.491* | 0.550* |
| 35 | LysoPE(0:0/18:3(6Z,9Z,12Z)) | 475.27 | 10.080 | 1.324* | 1.556* |
| 36 | LysoPE(0:0/18:2(9Z,12Z)) | 477.29 | 10.467 | 1.348 | 1.509* |
| 37 | LysoPE(0:0/20:4(5Z,8Z,11Z,14Z)) | 501.29 | 10.522 | 1.247* | 1.510* |
| 38 | PE(14:0/18:2(9Z,12Z)) | 687.48 | 14.375 | 0.590 | 0.358* |
| 39 | PC(14:0/P-16:0) | 689.54 | 14.707 | 0.474* | 0.329* |
| 40 | PE(14:0/20:5(5Z,8Z,11Z,14Z,17Z)) | 709.47 | 14.065 | 0.531 | 0.490* |
| 41 | PE(14:0/20:3(5Z,8Z,11Z)) | 713.50 | 14.521 | 0.571 | 0.424* |

604

605

Table 3 KEGG Metabolism Pathway of DEGs in the flesh of carp during different STMFPS treatments

| Pathway | The number of DEGs | | | All-gene | Pathway ID | Level 1 |
|---|--------------------|-------------|-------------|----------|------------|--------------------------------------|
| | Ctr vs. 1 d | Ctr vs. 5 d | Ctr vs. 9 d | | | |
| Metabolic pathways | 503 | 1163 | 1040 | 4521 | ko01100 | Global and overview maps |
| Purine metabolism | 83 | 194 | 168 | 807 | ko00230 | Nucleotide metabolism |
| Pyrimidine metabolism | 61 | 136 | 118 | 440 | ko00240 | Nucleotide metabolism |
| Glycerophospholipid metabolism | 44 | 107 | 92 | 424 | ko00564 | Lipid metabolism |
| Lysine degradation | 41 | 91 | 89 | 371 | ko00310 | Amino acid metabolism |
| N-Glycan biosynthesis | 49 | 87 | 72 | 227 | ko00510 | Glycan biosynthesis and metabolism |
| Oxidative phosphorylation | 28 | 87 | 52 | 332 | ko00190 | Energy metabolism |
| Inositol phosphate metabolism | 40 | 80 | 82 | 345 | ko00562 | Carbohydrate metabolism |
| Carbon metabolism | 33 | 78 | 78 | 393 | ko01200 | Global and overview maps |
| Glycerolipid metabolism | 24 | 62 | 51 | 206 | ko00561 | Lipid metabolism |
| Sphingolipid metabolism | 25 | 61 | 44 | 204 | ko00600 | Lipid metabolism |
| Amino sugar and nucleotide sugar metabolism | 19 | 56 | 43 | 188 | ko00520 | Carbohydrate metabolism |
| Arginine and proline metabolism | 18 | 53 | 43 | 224 | ko00330 | Amino acid metabolism |
| Cysteine and methionine metabolism | 19 | 52 | 41 | 192 | ko00270 | Amino acid metabolism |
| Ether lipid metabolism | 24 | 49 | 43 | 191 | ko00565 | Lipid metabolism |
| Arachidonic acid metabolism | 19 | 47 | 39 | 205 | ko00590 | Lipid metabolism |
| Biosynthesis of amino acids | 20 | 47 | 39 | 213 | ko01230 | Global and overview maps |
| Glutathione metabolism | 13 | 45 | 44 | 194 | ko00480 | Metabolism of other amino acids |
| Mannose type O-glycan biosynthesis | 28 | 38 | 41 | 97 | ko00515 | Glycan biosynthesis and metabolism |
| Glycolysis / Gluconeogenesis | 13 | 38 | 0 | 196 | ko00010 | Carbohydrate metabolism |
| Other types of O-glycan biosynthesis | 23 | 37 | 39 | 108 | ko00514 | Glycan biosynthesis and metabolism |
| Pyruvate metabolism | 13 | 35 | 38 | 174 | ko00620 | Carbohydrate metabolism |
| Fatty acid metabolism | 13 | 34 | 34 | 185 | ko01212 | Global and overview maps |
| Retinol metabolism | 15 | 33 | 31 | 146 | ko00830 | Metabolism of cofactors and vitamins |
| Porphyrin and chlorophyll metabolism | 14 | 33 | 28 | 97 | ko00860 | Metabolism of cofactors and vitamins |
| Valine, leucine and isoleucine degradation | 13 | 33 | 28 | 116 | ko00280 | Amino acid metabolism |
| Tryptophan metabolism | 10 | 32 | 33 | 118 | ko00380 | Amino acid metabolism |
| Fructose and mannose metabolism | 10 | 32 | 32 | 116 | ko00051 | Carbohydrate metabolism |

| | | | | | | |
|---|----|----|----|-----|---------|---|
| Glycosaminoglycan biosynthesis - heparan sulfate / heparin | 14 | 31 | 30 | 116 | ko00534 | Glycan biosynthesis and metabolism Xenobiotics |
| Drug metabolism - cytochrome P450 | 7 | 30 | 30 | 125 | ko00982 | biodegradation and metabolism Xenobiotics |
| Glycosphingolipid biosynthesis - lacto and neolacto series | 10 | 28 | 27 | 124 | ko00601 | Glycan biosynthesis and metabolism |
| Alanine, aspartate and glutamate metabolism | 11 | 28 | 25 | 122 | ko00250 | Amino acid metabolism |
| Nicotinate and nicotinamide metabolism | 9 | 27 | 28 | 112 | ko00760 | Metabolism of cofactors and vitamins Xenobiotics |
| Drug metabolism - other enzymes | 15 | 26 | 29 | 130 | ko00983 | biodegradation and metabolism Xenobiotics |
| Metabolism of xenobiotics by cytochrome P450 | 10 | 26 | 28 | 124 | ko00980 | biodegradation and metabolism |
| Citrate cycle (TCA cycle) | 7 | 26 | 25 | 143 | ko00020 | Carbohydrate metabolism |
| One carbon pool by folate | 11 | 25 | 28 | 156 | ko00670 | Metabolism of cofactors and vitamins |
| Other glycan degradation | 13 | 25 | 24 | 60 | ko00511 | Glycan biosynthesis and metabolism |
| Glyoxylate and dicarboxylate metabolism | 8 | 24 | 34 | 132 | ko00630 | Carbohydrate metabolism |
| Steroid hormone biosynthesis | 12 | 24 | 26 | 133 | ko00140 | Lipid metabolism |
| Pentose phosphate pathway | 13 | 24 | 19 | 95 | ko00030 | Carbohydrate metabolism |
| Glycosaminoglycan biosynthesis-chondroitin sulfate/dermatan sulfate | 12 | 24 | 18 | 105 | ko00532 | Glycan biosynthesis and metabolism Xenobiotics |
| Drug metabolism - cytochrome P450 | 7 | 30 | 30 | 125 | ko00982 | biodegradation and metabolism Xenobiotics |
| Glycosphingolipid biosynthesis - lacto and neolacto series | 10 | 28 | 27 | 124 | ko00601 | Glycan biosynthesis and metabolism |
| Alanine, aspartate and glutamate metabolism | 11 | 28 | 25 | 122 | ko00250 | Amino acid metabolism |
| Nicotinate and nicotinamide metabolism | 9 | 27 | 28 | 112 | ko00760 | Metabolism of cofactors and vitamins Xenobiotics |
| Drug metabolism - other enzymes | 15 | 26 | 29 | 130 | ko00983 | biodegradation and metabolism Xenobiotics |
| Metabolism of xenobiotics by cytochrome P450 | 10 | 26 | 28 | 124 | ko00980 | biodegradation and metabolism |
| Citrate cycle (TCA cycle) | 7 | 26 | 25 | 143 | ko00020 | Carbohydrate metabolism |
| One carbon pool by folate | 11 | 25 | 28 | 156 | ko00670 | Metabolism of cofactors and vitamins |

| | | | | | | |
|---|----|----|----|-----|---------|--|
| Other glycan degradation | 13 | 25 | 24 | 60 | ko00511 | Glycan biosynthesis and metabolism |
| Glyoxylate and dicarboxylate metabolism | 8 | 24 | 34 | 132 | ko00630 | Carbohydrate metabolism |
| Steroid hormone biosynthesis | 12 | 24 | 26 | 133 | ko00140 | Lipid metabolism |
| Pentose phosphate pathway | 13 | 24 | 19 | 95 | ko00030 | Carbohydrate metabolism |
| Glycosaminoglycan biosynthesis - chondroitin sulfate / dermatan sulfate | 12 | 24 | 18 | 105 | ko00532 | Glycan biosynthesis and metabolism |
| Mucin type O-glycan biosynthesis | 13 | 23 | 21 | 119 | ko00512 | Glycan biosynthesis and metabolism |
| Fatty acid degradation | 10 | 23 | 16 | 132 | ko00071 | Lipid metabolism |
| Glycosylphosphatidylinositol (GPI)-anchor biosynthesis | 12 | 22 | 26 | 85 | ko00563 | Glycan biosynthesis and metabolism |
| Glycine, serine and threonine metabolism | 7 | 22 | 25 | 114 | ko00260 | Amino acid metabolism |
| Terpenoid backbone biosynthesis | 12 | 22 | 21 | 54 | ko00900 | Metabolism of terpenoids and polyketides |
| Galactose metabolism | 5 | 19 | 14 | 113 | ko00052 | Carbohydrate metabolism |
| Pentose and glucuronate interconversions | 8 | 18 | 20 | 79 | ko00040 | Carbohydrate metabolism |
| Tyrosine metabolism | 7 | 18 | 19 | 90 | ko00350 | Amino acid metabolism |
| Propanoate metabolism | 11 | 18 | 17 | 90 | ko00640 | Carbohydrate metabolism |
| Starch and sucrose metabolism | 4 | 18 | 17 | 128 | ko00500 | Carbohydrate metabolism |
| Selenocompound metabolism | 8 | 17 | 12 | 39 | ko00450 | Metabolism of other amino acids |
| alpha-Linolenic acid metabolism | 8 | 17 | 10 | 91 | ko00592 | Lipid metabolism |
| Fatty acid elongation | 3 | 15 | 18 | 92 | ko00062 | Lipid metabolism |
| Glycosphingolipid biosynthesis - globo and isoglobo series | 4 | 15 | 14 | 69 | ko00603 | Glycan biosynthesis and metabolism |
| Linoleic acid metabolism | 6 | 15 | 12 | 88 | ko00591 | Lipid metabolism |
| Histidine metabolism | 5 | 14 | 12 | 53 | ko00340 | Amino acid metabolism |
| beta-Alanine metabolism | 12 | 13 | 19 | 86 | ko00410 | Metabolism of other amino acids |
| Ascorbate and aldarate metabolism | 6 | 13 | 17 | 70 | ko00053 | Carbohydrate metabolism |
| Fatty acid biosynthesis | 5 | 13 | 16 | 68 | ko00061 | Lipid metabolism |
| Pantothenate and CoA biosynthesis | 8 | 13 | 14 | 53 | ko00770 | Metabolism of cofactors and vitamins |
| Glycosphingolipid biosynthesis-ganglio series | 5 | 13 | 13 | 73 | ko00604 | Glycan biosynthesis and metabolism |
| Glycosaminoglycan degradation | 4 | 12 | 19 | 62 | ko00531 | Glycan biosynthesis and metabolism |
| Butanoate metabolism | 5 | 12 | 11 | 48 | ko00650 | Carbohydrate metabolism |
| Folate biosynthesis | 1 | 12 | 11 | 45 | ko00790 | Metabolism of cofactors and vitamins |
| Sulfur metabolism | 3 | 12 | 9 | 38 | ko00920 | Energy metabolism |
| Primary bile acid biosynthesis | 7 | 11 | 14 | 57 | ko00120 | Lipid metabolism |
| Biosynthesis of unsaturated fatty acids | 4 | 11 | 13 | 79 | ko01040 | Lipid metabolism |
| Glycosaminoglycan biosynthesis - keratan sulfate | 4 | 11 | 13 | 91 | ko00533 | Glycan biosynthesis and metabolism |

| | | | | | | |
|---|---|----|----|----|---------|---|
| Steroid biosynthesis | 3 | 11 | 8 | 56 | ko00100 | Lipid metabolism |
| Thiamine metabolism | 2 | 11 | 7 | 50 | ko00730 | Metabolism of cofactors and vitamins |
| Phenylalanine metabolism | 7 | 10 | 12 | 42 | ko00360 | Amino acid metabolism |
| Ubiquinone and other terpenoid-quinone biosynthesis | 3 | 10 | 11 | 30 | ko00130 | Metabolism of cofactors and vitamins |
| Arginine biosynthesis | 3 | 10 | 9 | 64 | ko00220 | Amino acid metabolism |
| Riboflavin metabolism | 6 | 10 | 8 | 24 | ko00740 | Metabolism of cofactors and vitamins |
| Phosphonate and phosphinate metabolism | 2 | 9 | 10 | 71 | ko00440 | Metabolism of other amino acids |
| 2-Oxocarboxylic acid metabolism | 1 | 7 | 5 | 54 | ko01210 | Global and overview maps |
| Taurine and hypotaurine metabolism | 4 | 6 | 8 | 42 | ko00430 | Metabolism of other amino acids |
| Vitamin B6 metabolism | 2 | 5 | 7 | 16 | ko00750 | Metabolism of cofactors and vitamins |
| Synthesis and degradation of ketone bodies | 1 | 4 | 5 | 13 | ko00072 | Lipid metabolism |
| Phenylalanine, tyrosine and tryptophan biosynthesis | 2 | 4 | 4 | 18 | ko00400 | Amino acid metabolism |
| Valine, leucine and isoleucine biosynthesis | 0 | 4 | 2 | 11 | ko00290 | Amino acid metabolism |
| Nitrogen metabolism | 1 | 3 | 11 | 56 | ko00910 | Energy metabolism |
| D-Glutamine and D-glutamate metabolism | 1 | 3 | 3 | 16 | ko00471 | Metabolism of other amino acids |
| Monobactam biosynthesis | 1 | 3 | 1 | 7 | ko00261 | Biosynthesis of other secondary metabolites |
| Biotin metabolism | 1 | 2 | 2 | 9 | ko00780 | Metabolism of cofactors and vitamins |
| Insect hormone biosynthesis | 1 | 2 | 2 | 14 | ko00981 | Metabolism of terpenoids and polyketides |
| C5-Branched dibasic acid metabolism | 0 | 2 | 0 | 6 | ko00660 | Carbohydrate metabolism |
| Lipoic acid metabolism | 0 | 1 | 2 | 8 | ko00785 | Metabolism of cofactors and vitamins |
| Caffeine metabolism | 2 | 1 | 1 | 8 | ko00232 | Biosynthesis of other secondary metabolites |
| D-Arginine and D-ornithine metabolism | 0 | 1 | 1 | 6 | ko00472 | Metabolism of other amino acids |
| Neomycin, kanamycin and gentamicin biosynthesis | 1 | 1 | 1 | 13 | ko00524 | Biosynthesis of other secondary metabolites |
| Polyketide sugar unit biosynthesis | 0 | 1 | 0 | 2 | ko00523 | Metabolism of terpenoids and polyketides |

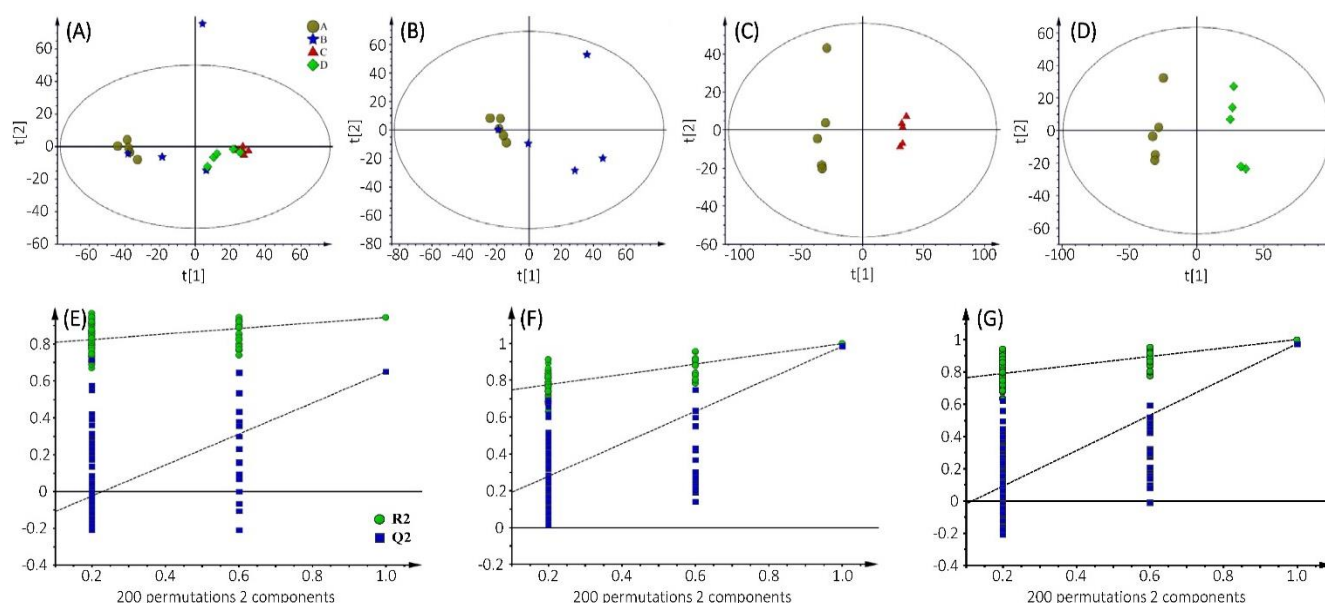
608

609

Table 4: DEGs related to ornithine cycle in crucian carp muscle during depuration

| Genetic code | Pathway No. | DEGs ^a | | | Expression of enzymes | Metabolites |
|--------------|----------------|-------------------|------|------|---|--|
| | | 1 d | 5 d | 9 d | | |
| 109070501 | k01940 | +1.0 | +2.7 | ND | argininosuccinate synthase [EC:6.3.4.5] | citruiline to arginosuccinate |
| 109058290 | k21121 | ND | +1.4 | +1.2 | N-alpha-acetyltransferase [EC:2.3.1.259] | glutamate to N- acteyl-glutamate |
| 109045545 | k01755 | ND | +1.7 | +1.0 | argininosuccinate lyase [EC:4.3.2.1] | arginosuccinate to arginine |
| 109056660 | k12657 | +1.2 | +1.8 | +1.4 | delta-1-pyrroline-5-carboxylate synthetase [EC:2.7.2.11]/[1.2.1.41] | glutamate to glutamate 5- semialdehyde |
| 109088420 | k00819 | ND | -2.1 | -2.3 | ornithine--oxo-acid transaminase [EC:2.6.1.13] | ornithine to glutamate 5- semialdehyde |
| 109113777 | k00286 | ND | +1.3 | +1.3 | pyrroline-5-carboxylate reductase [EC:1.5.1.2] | proline to 1- pyrroline-5- carboxylate |
| 109054371 | k11540 | ND | +1.1 | +1.1 | carbamoyl-phosphate synthase [EC:6.3.5.5] | glutamine to carbomyl- phosphate |

(Note, ^a value is presented as the differential expression multiple after log2 conversion. Positive value indicates that the sample group was up-regulated compared with the control group (depurated for 0 day). Negative value shows that the sample group was down-regulated compared with the control group (depurated for 0 day).)



031

Fig. 1 Results of PCA analysis (A-D) and the permutation test plots (E-G) from the OPLS-DA models for the metabolites obtained from crucian carp muscle during different depuration periods and detected using UPLC-QTOF/MS in both ionization modes. *Note: A: All samples in four groups; B: Control group vs. 1 d group; C: Control group vs. 5 d group; D: Control group vs. 9 d group; E: Control group vs. 1 d group; F: Control group vs. 5 d group; G: Control group vs. 9 d group. The criteria for validity of the OPLS-DA model are indicated as following: All blue Q^2 -values to the left are lower than the original points to the right; or the blue regression line of the Q^2 -points intersected the vertical axis (on the left) or below zero.*

640

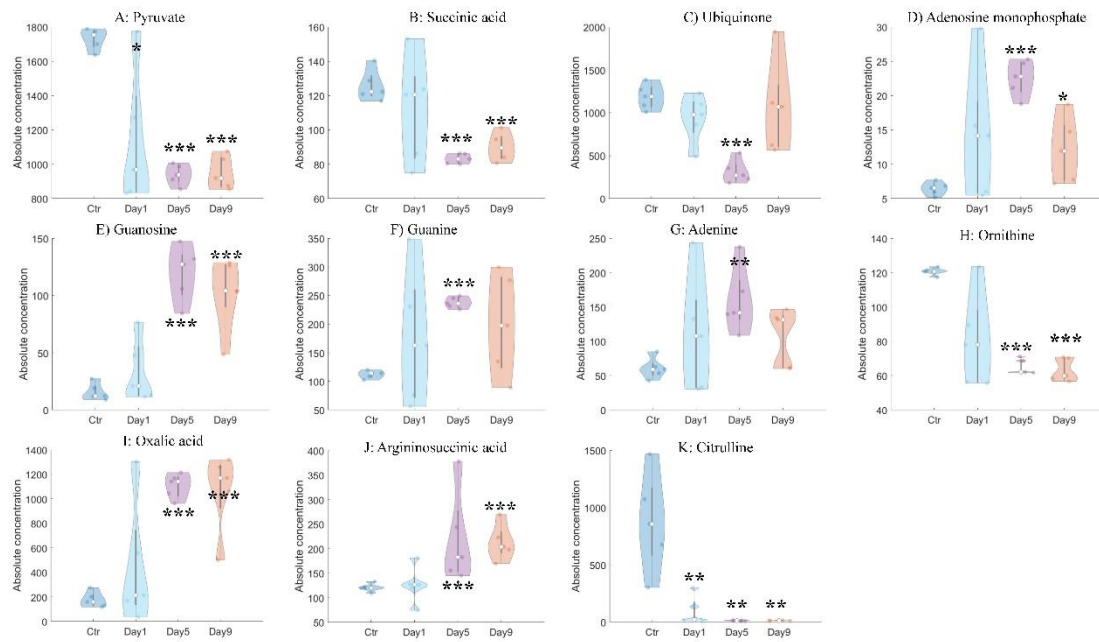


Fig. 2: Comparative contents of different metabolites in crucian carp muscle during the depuration procedure (*: <0.05; **: p<0.01; ***: p<0.001). Note: A-D: Related with energy metabolism; E-H: Related with the purine metabolic cycle; I-K: Related with the ornithine metabolic cycle.

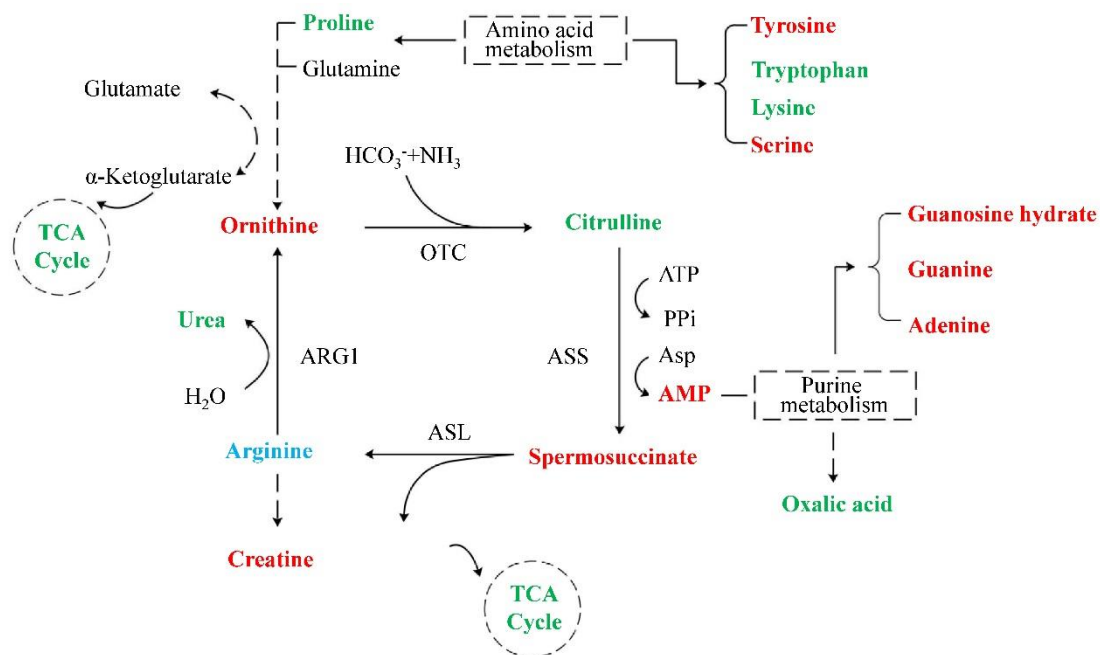


Fig. 3 Effect of depuration on metabolic pathways of crucian carp muscle. Note: *Different colors of metabolites represent change of comparative content, red: increased; blue: did not significantly change; green: decreased.*

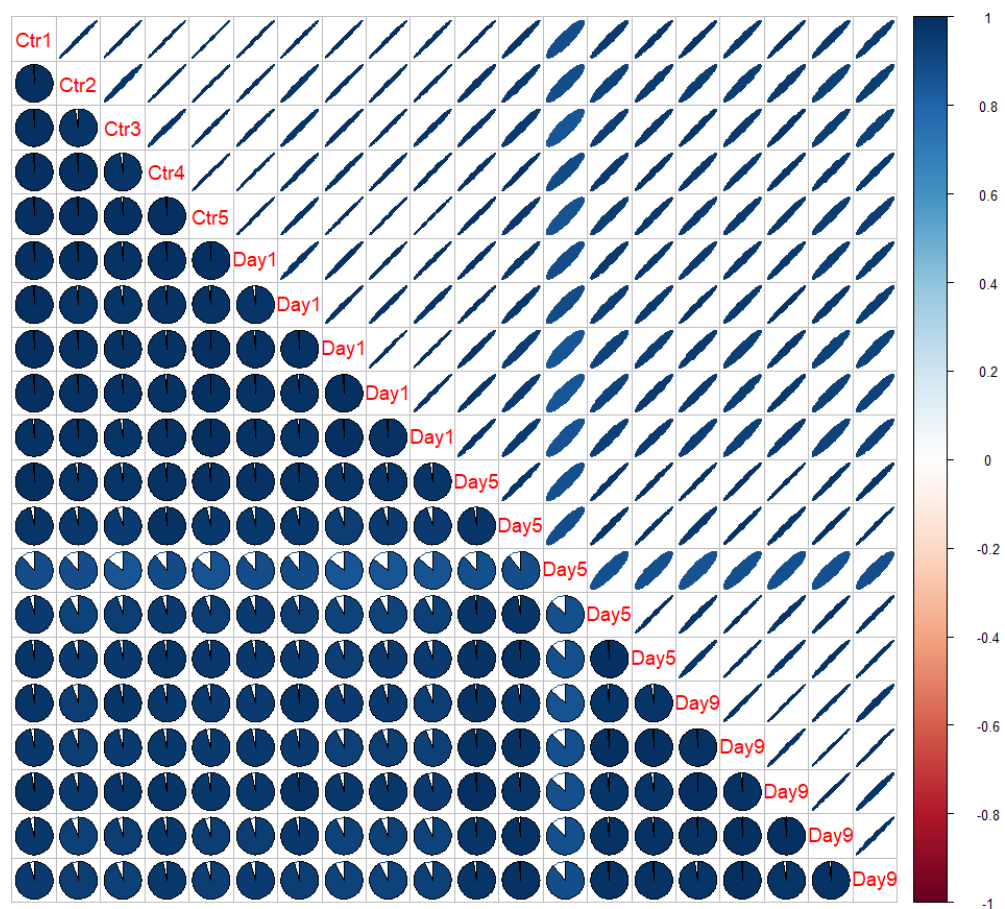


Fig. 4 Correlation heatmap of the Pearson correlation coefficient of all gene expressions in four different groups (Ctr1-Ctr5: Control; Day1: 1 d; Day5: 5 d; Day9: 9 d).

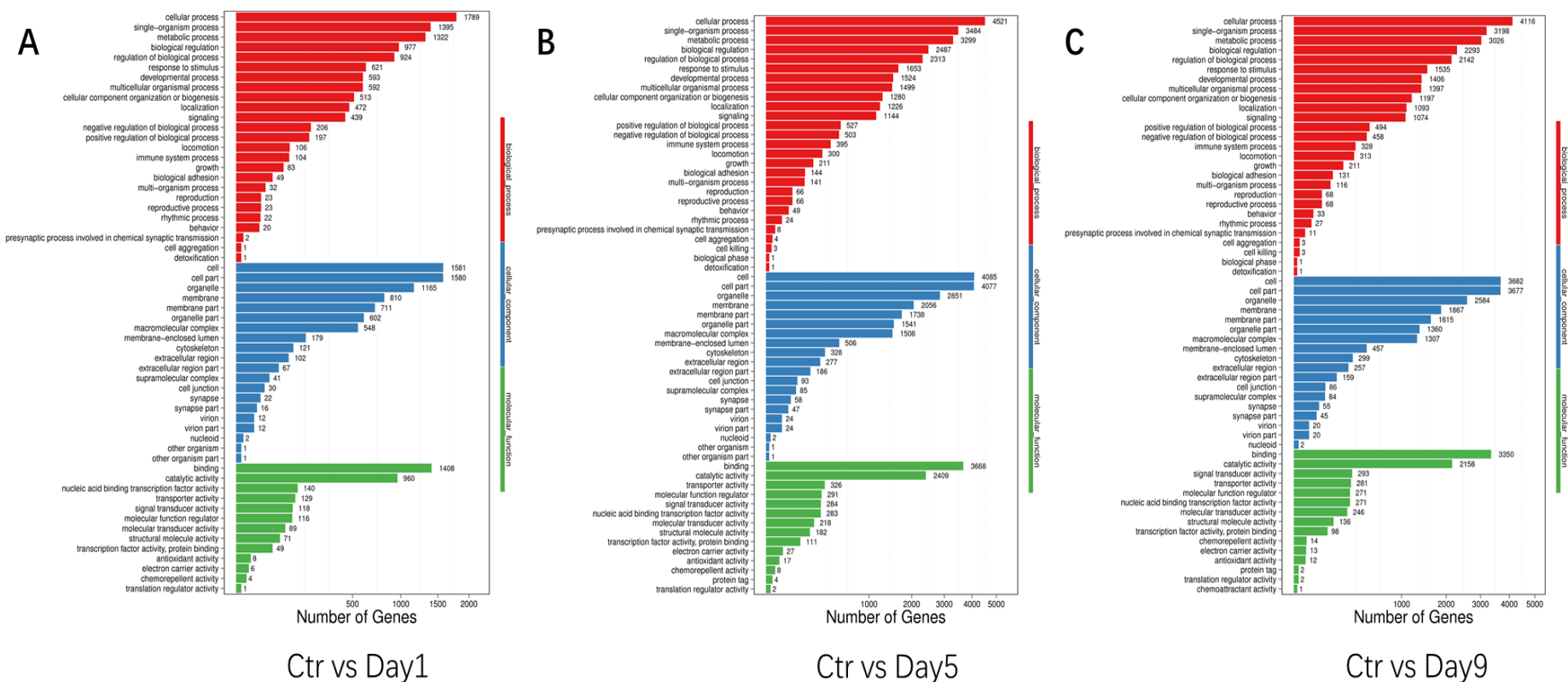


Fig. 6 GO classification of DEGs. (A) GO functional classification of DEGs between the control (Ctr) and Day1. (B) GO functional classification of DEGs between Ctr and Day5. (C) GO functional classification of DEGs between the Ctr and Day9. (Ctr, Day1, Day5, Day9 represent 0 d, 1 d, 5 d and 9 d STMFPS treated groups, respectively).